

Dynamical Decoupling of Quantum Two-Level Systems by Coherent Multiple Landau-Zener Transitions

Shlomi Matityahu,^{1,2,3,*} Hartmut Schmidt,⁴ Alexander Bilmes,⁴ Alexander Shnirman,^{3,5}

Georg Weiss,⁴ Alexey V. Ustinov,^{4,6} Moshe Schechter,¹ and Jürgen Lisenfeld⁴

¹*Department of Physics, Ben-Gurion University of the Negev, Beer Sheva 84105, Israel*

²*Department of Physics, Nuclear Research Centre-Negev, Beer-Sheva 84190, Israel*

³*Institute of Nanotechnology, Karlsruhe Institute of Technology, D-76344 Eggenstein-Leopoldshafen, Germany*

⁴*Physikalisches Institut, Karlsruhe Institute of Technology (KIT), 76131 Karlsruhe, Germany*

⁵*Institut für Theorie der Kondensierten Materie, KIT, 76131 Karlsruhe, Germany*

⁶*Russian Quantum Center, National University of Science and Technology MISIS, Moscow 119049, Russia*

(Dated: June 14, 2022)

Increasing and stabilizing the coherence of superconducting quantum circuits and resonators is of utmost importance for various technologies ranging from quantum information processors to highly sensitive detectors of low-temperature radiation in astrophysics. A major source of noise in such devices is a bath of two-level systems (TLSs) with broad distribution of energies, existing in disordered dielectrics and on surfaces. Here we study the dielectric loss of superconducting resonators in the presence of a periodic bias field, which sweeps near-resonant TLSs in and out of resonance with the resonator, resulting in a periodic pattern of Landau-Zener transitions. We show that at high sweep rates compared to the TLS relaxation rate, the coherent evolution of the TLS over multiple transitions yields a significant decrease in the dielectric loss. This behavior is observed both in the classical high-power regime and in the quantum single-photon regime, suggesting a viable technique to dynamically decouple TLSs from a qubit.

INTRODUCTION

Superconducting quantum devices are nowadays at the heart of many physical platforms exploring both foundations and applications of quantum mechanics. In particular, superconducting quantum circuits [1] are one of the prime contenders for the realization of a quantum computer [2, 3], and superconducting microwave resonators are of great interest for photon detection in astronomy applications [4, 5]. The coupling of superconducting qubits to resonators provides exciting prospects for studying quantum optics and atomic physics in an engineerable architecture with strong nonlinearities and interactions [6–8].

Originally postulated in the 1970's to explain the low-temperature properties of amorphous solids [9, 10], tunneling two-level systems (TLSs) have attracted a lot of renewed interest in the field of superconducting quantum devices, where such defects residing in the amorphous oxides of the microfabricated circuits form a major energy relaxation and decoherence channel [11]. Since TLSs couple both to strain and electric fields, those that are in resonance with a device electromagnetic mode efficiently dissipate electromagnetic energy into phonon excitations, giving rise to dielectric loss in superconducting microwave resonators and energy relaxation in superconducting qubits. Moreover, due to mutual TLS-TLS interactions [12], the thermal fluctuations of low-frequency TLSs give rise to fluctuations of high-frequency resonant TLSs — a phenomenon known as spectral diffusion, which causes time-dependent fluctuations of the device's electromagnetic environment [13–19]. Improv-

ing and stabilizing the coherence properties of superconducting devices is crucial for the realization of a scalable quantum computer [2, 3].

In the standard tunneling model [9, 10], each TLS is described by the Hamiltonian

$$\mathcal{H} = \frac{1}{2}(\Delta\sigma_z + \Delta_0\sigma_x) + \left(\sum_{\alpha,\beta}\gamma_{\alpha\beta}\varepsilon_{\alpha\beta} - \mathbf{p} \cdot \mathbf{E}\right)\sigma_z, \quad (1)$$

where σ_x and σ_z are the Pauli matrices, Δ and Δ_0 are the bias and tunneling energies of the unperturbed TLS, and $\gamma_{\alpha\beta} \equiv (1/2)\partial\Delta/\partial\varepsilon_{\alpha\beta}$, $\mathbf{p} \equiv (1/2)\partial\Delta/\partial\mathbf{E}$ are the elastic quadrupole and electric dipole moments of the TLS, which couple to the strain and electric fields $\varepsilon_{\alpha\beta}$ and \mathbf{E} . The distribution of Δ and Δ_0 is quite universal and has the form $f(\Delta, \Delta_0) = P_0/\Delta_0$, with P_0 being a material dependent constant.

For strongly driven superconducting microwave resonators at low temperatures, $k_B T \ll \hbar\omega$, interaction of the resonator electric field $\mathbf{E}_{\text{res}}(t) = \mathbf{E}_{\text{ac}} \cos(\omega t)$ with resonant TLSs leads to the well-known expression for the dielectric loss tangent (inverse quality factor) [20], $\tan \delta = \tan \delta_0 / \sqrt{1 + \Omega_{\text{R0}}^2 T_1 T_2}$, where $\tan \delta_0 = \pi P_0 p^2 \tanh(\hbar\omega/2k_B T)/(3\epsilon)$ is the intrinsic loss tangent in the low-power limit (ϵ is the dielectric constant) [21], $\Omega_{\text{R0}} = pE_{\text{ac}}/\hbar$ is the TLS maximum Rabi frequency and T_1, T_2 are characteristic TLS relaxation and decoherence times. This power dependence arises from saturation of individual TLSs. Unfortunately, using this saturation effect to improve the coherence times of superconducting qubits is impractical, as unwanted qubit excitations are caused either by the applied strong resonant field or by excited TLSs via the qubit-TLS interaction.

Recently, the dielectric loss of superconducting resonators was studied in the presence of a periodic bias field $\mathbf{E}_{\text{bias}}(t)$, which slowly changes the bias energy of TLSs at a (maximum) rate $v_0 = 2p\dot{E}_{\text{bias}}$, and sweeps them through resonance with the resonator [22, 23]. The dynamics of each transition is of the Landau-Zener (LZ) type [24–26], with a non-adiabatic transition probability

$$P = e^{-1/\xi}, \quad (2)$$

where $\xi = 2|v_0|/(\pi\hbar\Omega_{\text{R0}}^2)$ is a dimensionless parameter. At slow sweep rates $|v_0| \ll \hbar\Omega_{\text{R0}}\Gamma_1$ (or $\xi \ll \xi_1 \equiv \Gamma_1/\Omega_{\text{R0}}$), the transition time for a single LZ transition, $t_{\text{LZ}} = \hbar\Omega_{\text{R0}}/|v_0|$, is longer than the TLS relaxation time T_1 ; the LZ transitions are irrelevant, and the loss tangent is almost independent of the sweep rate and given by the non-linear saturation discussed above. For $\hbar\Omega_{\text{R0}}\Gamma_1 \ll |v_0| \ll \hbar\Omega_{\text{R0}}^2$ ($\xi_1 \ll \xi \ll 1$), each LZ transition is coherent and adiabatic, with photon absorption probability $1 - P \approx 1$, meaning that each TLS swept through resonance dissipates one photon. As the number of TLSs swept through resonance is proportional to $|v_0|$, the loss increases linearly with $|v_0|$. In the regime $|v_0| \gg \hbar\Omega_{\text{R0}}^2$ ($\xi \gg 1$) each transition becomes non-adiabatic, leading to a universal constant loss tangent independent of the resonator field, which is equal to the low-power limit $\tan \delta_0$ [23]. This is a consequence of short transition time t_{LZ} compared to the Rabi oscillation period Ω_{R0}^{-1} , such that resonant TLSs are unsaturated at any instant.

A crucial assumption of the results described above is the long period of the bias field, T_{sw} , compared to the relaxation time T_1 . In this regime, TLSs relax after each transition, and two subsequent transitions are independent. Here, we explore higher sweep rates $T_{\text{sw}} < T_1$, where the coherent evolution during several LZ transitions has to be considered. We show theoretically and experimentally that due to interference effects, the resonator loss decreases again in this regime. In contrast to the low dielectric loss at zero sweep rate, arising from saturation of photon absorption by TLSs for $\Omega_{\text{R0}} \gg \Gamma_1$, the low loss in the high sweep rate regime $T_{\text{sw}}^{-1} \gg \Gamma_1$ is a consequence of a reduced photon absorption probability due to destructive interference between many LZ transitions. In contrast to strong resonant driving in the saturation regime $\Omega_{\text{R0}} \gg \Gamma_1$, the reduction of the loss in the high sweep rate regime $T_{\text{sw}}^{-1} \gg \Gamma_1$ is achieved by application of time-dependent bias fields with frequency spectrum lower than the resonance frequency ω . We also discuss the single-photon regime, and show experimental evidence for the applicability of the theory in this regime. Since the physics of the single-photon regime is equivalent to that of a qubit coupled to a resonant TLS, the results suggest a technique to effectively decouple near-resonant TLSs from a qubit without affecting the qubit state.

SUPPRESSION OF TLS DIELECTRIC LOSS IN MICROWAVE RESONATORS

Theory

We consider a TLS with the Hamiltonian (1) in the presence of the resonator field $\mathbf{E}_{\text{res}}(t) = \mathbf{E}_{\text{ac}} \cos(\omega t)$ and a parallel periodic bias field $\mathbf{E}_{\text{bias}}(t)$ with period T_{sw} , satisfying $\mathbf{E}_{\text{bias}}(0) = \mathbf{E}_{\text{bias}}(T_{\text{sw}}) = 0$ and having a maximum value E_{max} . This bias field shifts the TLS bias energy, such that $\Delta(t) = \Delta(0) - 2\mathbf{p} \cdot \mathbf{E}_{\text{bias}}(t)$. Under these assumptions, a number $n_{\text{TLS}} \approx P_0 p E_{\text{max}}$ of TLSs per unit volume are swept into resonance with the resonator field in each period of the bias field. In a single period, most of these TLSs experience two LZ transitions during which dissipation is negligible for $\xi \gg \xi_1 = \Gamma_1/\Omega_{\text{R0}}$; the TLS dynamics in each resonance, occurring at time t_0 for which the TLS energy splitting $\mathcal{E}(t) = \sqrt{\Delta^2(t) + \Delta_0^2}$ equals $\hbar\omega$, is governed by the LZ Hamiltonian [27]

$$\mathcal{H}_{\text{LZ}}(t) = \frac{1}{2} [v(t - t_0)\sigma_z + \hbar\Omega_{\text{R}}\sigma_x]. \quad (3)$$

Here, σ_x and σ_z are the Pauli matrices in the diabatic basis $\{|g, n\rangle, |e, n-1\rangle\}$ ($|g\rangle$ and $|e\rangle$ being the TLS ground and excited states, respectively, and $|n\rangle$ is a photon number state) [27], and $v = v_0 \cos \eta \sqrt{1 - (\Delta_0/\hbar\omega)^2}$ is the TLS energy sweep rate, with $v_0 = 2p\dot{E}_{\text{bias}}(t_0)$ the maximum sweep rate and η the angle between the TLS dipole moment and the electric fields; the TLS Rabi frequency is $\Omega_{\text{R}} = \Omega_{\text{R0}}(\Delta_0/\mathcal{E}) \cos \eta$.

To obtain the dielectric loss due to TLSs, we calculate the counting statistics of the number of photons absorbed by a single TLS. Within the full counting statistics formalism, the evolution operator describing a single coherent LZ transition is [28]

$$\mathcal{U}_{\text{LZ}}(k) = \begin{pmatrix} \sqrt{P} & e^{i\frac{k}{2}} e^{-i\psi} \sqrt{1-P} \\ -e^{-i\frac{k}{2}} e^{i\psi} \sqrt{1-P} & \sqrt{P} \end{pmatrix}, \quad (4)$$

where ψ is the Stokes phase, approaching 0 and $\pi/4$ in the adiabatic ($\xi \ll 1$) and non-adiabatic ($\xi \gg 1$) limits, respectively [29]. Note that a sign reversal of v in the Hamiltonian (3) corresponds to the transformation $\psi \rightarrow \pi - \psi$ in Eq. (4) [27, 28]. The counting field k counts the number of photons absorbed by the TLS, with the factors $e^{-ik/2}$ and $e^{ik/2}$ corresponding to the absorption and emission of a photon. In Liouville space [27], this evolution operator transforms into the superoperator $U_{\text{LZ}}(k) = \mathcal{U}_{\text{LZ}}(k) \otimes [\mathcal{U}_{\text{LZ}}(-k)]^*$.

In between two successive transitions, the TLS is out of resonance for a time interval t and the dynamics of its density matrix ρ is described by the Lindblad equation,

$$\dot{\rho} = -\frac{i}{\hbar} [\mathcal{H}_{\text{TLS}}, \rho] + \sum_{i=\pm} \Gamma_i \left(L_i \rho L_i^\dagger - \frac{1}{2} \{L_i^\dagger L_i, \rho\} \right), \quad (5)$$

where $\mathcal{H}_{\text{TLS}}(t) = (\mathcal{E}(t)/2)\sigma_z$, $L_{\pm} = \sigma_{\pm} = (\sigma_x \pm i\sigma_y)/2$ and $\Gamma_{+} = \Gamma_{\uparrow}$, $\Gamma_{-} = \Gamma_{\downarrow}$ are the transition rates between the TLS eigenstates. For simplicity, we assume no pure dephasing, such that the decoherence rate is $\Gamma_2 = \Gamma_1/2$, where $\Gamma_1 = \Gamma_{\uparrow} + \Gamma_{\downarrow}$ is the relaxation rate. The corresponding evolution operator in Liouville space is [27]

$$U(t) = \begin{pmatrix} \frac{\Gamma_{\uparrow}}{\Gamma_1} + \frac{\Gamma_{\downarrow}}{\Gamma_1} e^{-\Gamma_1 t} & 0 & 0 & \frac{\Gamma_{\uparrow}}{\Gamma_1} (1 - e^{-\Gamma_1 t}) \\ 0 & e^{i\phi(t) - \Gamma_2 t} & 0 & 0 \\ 0 & 0 & e^{-i\phi(t) - \Gamma_2 t} & 0 \\ \frac{\Gamma_{\downarrow}}{\Gamma_1} (1 - e^{-\Gamma_1 t}) & 0 & 0 & \frac{\Gamma_{\downarrow}}{\Gamma_1} + \frac{\Gamma_{\uparrow}}{\Gamma_1} e^{-\Gamma_1 t} \end{pmatrix}, \quad (6)$$

where $\phi(t) = \frac{1}{\hbar} \int_0^t \mathcal{E}(t') dt'$. The evolution of the density matrix after one period of the bias field is obtained as $|\rho(T_{\text{sw}}, k)\rangle = U_{\text{sw}}(k) |\rho(0)\rangle$, where $|\rho\rangle = (\rho_{00}, \rho_{01}, \rho_{10}, \rho_{11})^T$ is the ket representing the density matrix ρ in Liouville space [27], and $U_{\text{sw}}(k) = U_{\text{LZ}}(\pi - \psi, k) U(t_2) U_{\text{LZ}}(\psi, k) U(t_1)$ with $T_{\text{sw}} = t_1 + t_2$ (here we have used the fact that the sweep velocity changes sign between consecutive transitions). The evolution after time $t = NT_{\text{sw}}$ is then

$$|\rho(t, k)\rangle = U_{\text{sw}}^N(k) |\rho(0)\rangle. \quad (7)$$

The generating function for the statistics of the TLS photon absorption after time $t = NT_{\text{sw}}$ is given by

$$\chi(t, k) = \text{Tr} [|\rho(t, k)\rangle] = \text{Tr} [U_{\text{sw}}^N(k) |\rho(0)\rangle], \quad (8)$$

where the trace operation is defined as $\text{Tr} [|\rho\rangle] \equiv \rho_{00} + \rho_{11}$. In particular, the number of photons absorbed by the TLS during time t is given by the first moment $\langle N_{\text{ph}}(t) \rangle = -i \frac{\partial \chi(t, k)}{\partial k} \Big|_{k=0}$. For $k = 0$ there should be a stationary solution to Eq. (7), meaning that one of the eigenvalues λ_1 of $U_{\text{sw}}(k=0)$ equals unity, whereas $|\lambda_i| < 1$ for $i = 2, 3, 4$. As a result, in the limit $t \rightarrow \infty$ only the mode with eigenvalue $\lambda_1 = 1$ will contribute, and after some algebra we obtain the photon absorption rate per TLS [27],

$$\gamma_{\text{abs}} = \lim_{t \rightarrow \infty} \frac{\langle N_{\text{ph}}(t) \rangle}{t} = -\frac{i}{T_{\text{sw}}} \langle g_1 | \frac{dU_{\text{sw}}}{dk} \Big|_{k=0} | v_1 \rangle, \quad (9)$$

where $\langle g_1 |$ and $| v_1 \rangle$ are the left and right eigenvectors of $U_{\text{sw}}(k=0)$ corresponding to the eigenvalue $\lambda_1 = 1$. The total photon absorption rate per unit volume is $\Gamma_{\text{abs}} = n_{\text{TLS}} \gamma_{\text{abs}} \approx P_0 p E_{\text{max}} \gamma_{\text{abs}}$. Comparing the power dissipation density $P_{\text{dis}} = -\hbar \omega \Gamma_{\text{abs}}$ with $P_{\text{dis}} = -\frac{1}{2} \omega \epsilon'' E_{\text{ac}}^2$, we obtain the expression for the loss tangent

$$\tan \delta = \frac{\epsilon''}{\epsilon'} = \frac{2\hbar \Gamma_{\text{abs}}}{\epsilon E_{\text{ac}}^2} = \frac{2p^2 \Gamma_{\text{abs}}}{\epsilon \hbar \Omega_{\text{R0}}^2}, \quad (10)$$

where ϵ' and ϵ'' are the real and imaginary parts of the dielectric constant.

The general expression for γ_{abs} is somewhat complicated, see [27]. Let us analyze it in simple limits, assuming low temperatures $k_{\text{B}} T \ll \hbar \omega$ for which $\Gamma_1 \approx$

Γ_{\downarrow} ($\Gamma_{\uparrow} \approx 0$). In the incoherent limit $\Gamma_1 T_{\text{sw}} \gg 1$, or $\xi \ll \xi_2$ with $\xi_2 \equiv 8pE_{\text{max}}\Gamma_1/(\pi\hbar\Omega_{\text{R0}}^2)$, we obtain $\gamma_{\text{abs}} \approx 2(1-P)/T_{\text{sw}}$. Equation (10) then gives the universal behavior discussed in Refs. [22, 23], namely $\tan \delta / \tan \delta_0 \approx 1$ in the non-adiabatic limit $\xi \gg 1$, and $\tan \delta / \tan \delta_0 \approx \xi$ for $\xi_1 \ll \xi \ll 1$ [27]. Thus, the results of Refs. [22, 23] are reproduced if subsequent LZ transitions are incoherent such that TLSs start from the ground state at each transition.

In the coherent regime $\Gamma_1 T_{\text{sw}} \ll 1$ or $\xi \gg \xi_2$, TLSs experience $M = (\Gamma_1 T_{\text{sw}})^{-1} = \xi/\xi_2 \gg 1$ multiple coherent transitions. In the non-adiabatic regime $\xi \gg 1$, where the probability $1 - P$ for photon absorption/emission in a single transition is small, the interference between multiple transitions is constructive for $\phi_1 + \phi_2 = 0$ [27], where $\phi_{1,2}$ are the dynamical phases accumulated between successive transitions. This gives rise to a resonance in γ_{abs} , whose width in the non-adiabatic regime $\xi \gg 1$ is $\delta\phi \propto M^{-1}$ for $M^2(1-P) < 1$ and $\delta\phi \propto \sqrt{1-P}$ for $M^2(1-P) > 1$ [27]. The contribution of TLSs out of resonance is $\gamma_{\text{abs}}^{\text{non-res}} \propto \Gamma_1(1-P)$, with weak dependence on ϕ_1 and ϕ_2 . Two different behaviors of the loss tangent in the coherent regime are expected for $\xi_2 \ll 1$ and $\xi_2 \gg 1$.

For $\xi_2 \ll 1$, the regime $\xi_2 \ll \xi \ll 1$ is coherent and adiabatic, meaning that photons are absorbed and re-emitted by the TLSs with high probability. The photons are thus dissipated at the relaxation rate of the TLSs, so that $\gamma_{\text{abs}} \propto \Gamma_1$ [27]. This gives rise to constant loss tangent, $\tan \delta \propto \xi_2$. The resonance width in the non-adiabatic regime $\xi_2 \ll 1 \ll \xi$ is $\delta\phi \propto \sqrt{1-P}$ (since $M^2(1-P) \approx \xi/\xi_2^2 \gg 1$), and its contribution to the photon absorption rate is $\gamma_{\text{abs}}^{\text{res}} \approx \gamma_{\text{abs}}(\phi_1 = -\phi_2) \cdot \delta\phi \propto \Gamma_1 \sqrt{1-P}$. Hence, the loss tangent decreases as $\xi^{-1/2}$.

For $\xi_2 \gg 1$, the loss tangent follows the universal plateau up to $\xi \sim \xi_2$. For $\xi \gg \xi_2^2$ the resonance width is again $\delta\phi \propto \sqrt{1-P}$, and the corresponding contribution to the loss tangent is again $\propto \xi^{-1/2}$. In the crossover region $\xi_2 \ll \xi \ll \xi_2^2$ the resonance width is $\delta\phi \propto M^{-1}$, giving rise to the photon absorption rate $\gamma_{\text{abs}}^{\text{res}} \approx \gamma_{\text{abs}}(\phi_1 = -\phi_2) \cdot \delta\phi \propto \Gamma_1 M(1-P)$, which depends weakly on ξ . Note that for both $\xi_2 \ll 1$ and $\xi_2 \gg 1$ the contribution of the resonance dominates over that of the off-resonance part.

The results for the loss tangent obtained by a numerical average of γ_{abs} over a homogeneous distribution of the phases ϕ_1 and ϕ_2 are shown in Fig. 1 [27]. For simplicity, we neglect the distribution of Δ_0 , p and η in all other quantities, such as the sweep rate, the Rabi frequency and the relaxation rate, and assume $t_1 = t_2 = T_{\text{sw}}/2$. One readily observes the qualitative limits discussed above.

We stress that the decrease of the loss at the coherent and non-adiabatic regime $\xi \gg \max\{1, \xi_2\}$ is a result of interference between M coherent LZ transitions, which

reduce the photon absorption probability. To see this, consider N identical TLSs of which $N_g(t)$ and $N_e(t)$ occupying the ground and excited states, respectively. In a classical approach, one can write a rate equation for $N_e(t)$,

$$\begin{aligned}\dot{N}_e &= \gamma(N_g - N_e) - \Gamma_\downarrow N_e + \Gamma_\uparrow N_g \\ &= \gamma(N - 2N_e) - \Gamma_\downarrow N_e + \Gamma_\uparrow N,\end{aligned}\quad (11)$$

where $\gamma = 2(1 - P)/T_{\text{sw}}$ is the photon emission and absorption rate in a single LZ transition. The steady state solution is $N_e = N(\gamma + \Gamma_\uparrow)/(2\gamma + \Gamma_\downarrow)$ and the corresponding photon absorption rate per TLS is

$$\gamma_{\text{abs}} = \frac{\gamma(N - 2N_e)}{N} = \frac{\Gamma_\downarrow - \Gamma_\uparrow}{\Gamma_\downarrow} \frac{\gamma}{1 + 2\gamma/\Gamma_\downarrow}.\quad (12)$$

Since $(\Gamma_\downarrow - \Gamma_\uparrow)/\Gamma_\downarrow = \tanh(\hbar\omega/2k_B T)$ equals unity at low temperatures, we obtain $\gamma_{\text{abs}} \approx \gamma$ for $\gamma \ll \Gamma_\downarrow$ (or $M(1 - P) \ll 1$) and $\gamma_{\text{abs}} \approx \Gamma_\downarrow/2$ for $\gamma \gg \Gamma_\downarrow$ (or $M(1 - P) \gg 1$). The first limit corresponds to the result of Refs. [22, 23] and the second limit corresponds to a constant loss tangent $\tan \delta \propto \xi_2$ as discussed above. Therefore, the classical approach does not capture the physics of the fast sweep regime, which exhibits a decreasing loss with increasing sweep rate.

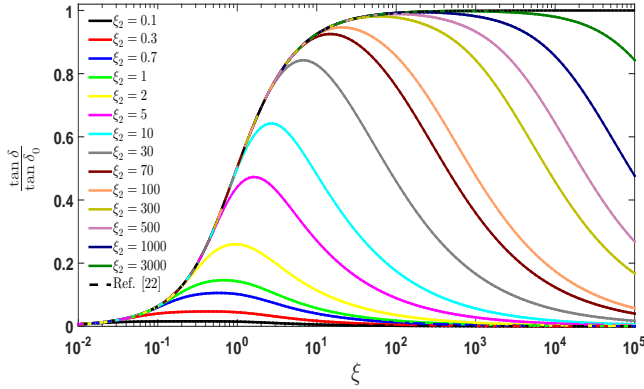


FIG. 1. Theoretical results for the loss tangent due to TLSs, normalized by the intrinsic low-power loss tangent $\tan \delta_0 = \pi P_0 p^2 / (3\epsilon)$, as a function of the dimensionless sweep rate $\xi \equiv 2|v_0|/(\pi \hbar \Omega_{R0}^2)$ for various values of $\xi_2 \equiv 8pE_{\text{max}}\Gamma_\downarrow/(\pi \hbar \Omega_{R0}^2)$, as indicated in the legend. The results are obtained by a numerical average of the photon absorption rate per TLS, $\langle \gamma_{\text{abs}} \rangle$, over a homogeneous distribution of the phases ϕ_1 and ϕ_2 . We neglect the distribution in Δ_0 , p and η in all other quantities, and assume $t_1 = t_2 = T_{\text{sw}}/2$.

Experiment

In our experiment, we study TLS in deposited aluminum oxide by using it as the dielectric in lumped-element LC-resonators. This material is highly relevant

for superconducting quantum processors, because it is used for tunnel barriers in Josephson junctions of qubits and also forms naturally on circuit wiring after air exposure. However, any depositable dielectric can in principle be studied with this method.

Figure 2 shows a sample resonator structured by optical lithography from superconducting aluminum on a sapphire substrate. Following experiments by Khalil et al. [23], the capacitances are designed as bridges consisting of four equal Al/AlO_x/Al capacitors. Hereby, an electric bias field can be applied to the dielectric. In addition, our setup allows for mechanical TLS tuning by controlling the strain in the sample material with a piezo actuator [12]. Each chip contains 8 slightly different resonators that are coupled to a common transmission line, and is installed in a well-shielded and heavily filtered cryogenic setup that allows for measurements in the single-photon regime at sample temperatures of 30 mK [30]. All capacitors contain a 25-nm thick layer of amorphous AlO_x that is deposited in a Plassys system by eBeam-evaporation of aluminum in a low-pressure oxygen atmosphere. Further details on the setup and fabrication are found in [27].

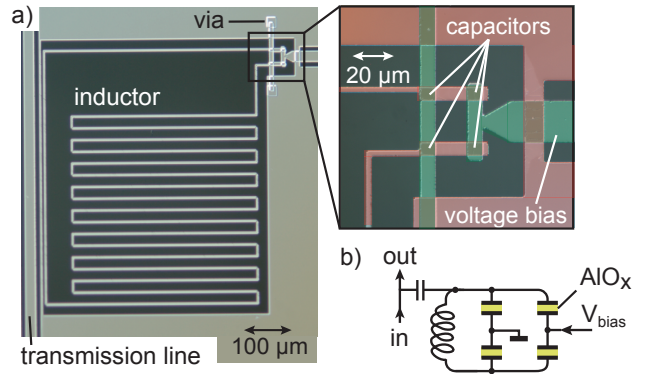


FIG. 2. a) Photograph of a lumped-element resonator consisting of a capacitively terminated meandering inductor. The (colorized) inset shows a zoom of the four capacitors between bottom (red) and top layers (green), which are separated by 25nm-thick amorphous AlO_x. b) Circuit schematic. The electric field in the capacitor dielectric is controlled by an applied bias voltage V_{bias} .

We characterize the total dielectric loss tangent $\tan \delta \equiv 1/Q_i$ by recording resonance curves using a network analyzer and extracting the internal quality factor Q_i using a standard fit procedure [31]. In particular, we study this loss while a triangular voltage signal $V_{\text{bias}}(t)$ is applied as a bias to the sample dielectric. This results in a sweep rate $v_0 = p\dot{V}_{\text{bias}}/d$, where $d = 25\text{ nm}$ is the distance between the capacitor plates, considering that due to the design only half the voltage drops at each capacitor. The maximum Rabi frequency is calculated as $\Omega_{R0} = pE_{\text{ac}}/\hbar = \sqrt{(p^2 P_{\text{in}} Q_l^2)/(\hbar^2 \omega C Q_c d^2)}$, where P_{in} is the input power, Q_l , Q_c are the measured loaded and coupling quality factors, C is the total resonator capac-

itance, and a typical value of $p = 0.5 \text{ e}\text{\AA}$ is used as an average dipole moment of TLS in AlO_x [11]. Note that for a given P_{in} , the value of E_{ac} (and thus Ω_{R0}) depends on the resonator loss (and thus on ξ). Below we estimate Ω_{R0} using the value of $\tan \delta$ in the absence of the bias field ($\xi = 0$).

Figure 3 shows the measured dielectric loss tangent in two different resonators as a function of the dimensionless sweep rate ξ , for several maximum values E_{max} of the bias field at a fixed input power. For the high value of Ω_{R0} in Fig. 3a), the corresponding values of ξ_2 are smaller than ~ 10 , and the data show a flat maximum for $\xi_2 \ll \xi < 1$ in the regime $\xi_2 \ll 1$, which evolves into a peak at $\xi = \xi_2$ with increasing ξ_2 , followed by a strong decrease. Using $\xi_2 \approx 1$ for the upper curve in Fig. 3a) and $p = 0.5 \text{ e}\text{\AA}$, we obtain $\Gamma_1 \approx 1 \text{ MHz}$, in accordance with TLS relaxation rates observed in AlO_x [32–34]. The data in Fig. 3b) correspond to a much lower value of Ω_{R0} , i.e., to values of $\xi_2 \gg 1$. As a result, one observes the universal plateau, followed by a strong decrease at $\xi \sim \xi_2^2$. Both these regimes are in excellent qualitative agreement with the numerical results in Fig. 1.

In Fig. 4 we show $\tan \delta$ as a function of the dimensionless sweep rate ξ for several input powers, at a fixed value of E_{max} . Here the values of Ω_{R0}^2 differ by an order of magnitude between subsequent curves, and therefore the value of ξ_2 is changed overall by five orders of magnitude. As a result, both regimes $\xi_2 \ll 1$ and $\xi_2 \gg 1$ are observed, exhibiting all the qualitative features predicted by the theoretical results in Fig. 1.

THE SINGLE-PHOTON REGIME AND EQUIVALENCE TO A QUBIT COUPLED TO RESONANT TLSS

To examine whether the effect discussed above is also applicable in the single-photon regime, we consider now a quantized single-mode cavity field $\mathbf{E}_{\text{res}}(t) = \hat{\mathbf{e}} \sqrt{\hbar \omega / \epsilon_0 V} (a e^{-i\omega t} + a^\dagger e^{i\omega t}) \sin(kz)$ ($\hat{\mathbf{e}}$ is a polarization unit vector, ϵ_0 the vacuum permittivity, V the resonator volume, k the wave vector, and a^\dagger , a the photon creation and annihilation operators) propagating along the z -axis and interacting with a set of near-resonant TLSs. After neglecting the longitudinal coupling and applying the rotating wave approximation, the corresponding Hamiltonian is

$$\mathcal{H} = \frac{1}{2} \sum_i \mathcal{E}_i \sigma_z^i + \hbar \omega a^\dagger a + \sum_i g_i (\sigma_+^i a + \sigma_-^i a^\dagger), \quad (13)$$

where $g_i = -p(\Delta_0 / \mathcal{E}_i) \sqrt{\hbar \omega / \epsilon_0 V} \sin(kz_i)$ and $\sigma_\pm = (\sigma_x \pm i\sigma_y)/2$. As the last term couples different TLSs via the quantized cavity field, the assumption of independent TLSs cannot be invoked as in the case of a classical field discussed above (which corresponds to the substitution $2g_i \sqrt{n_{\text{ph}}} = \Omega_{\text{R},i}$). For $\langle n_{\text{ph}} \rangle \gg 1$, each TLS

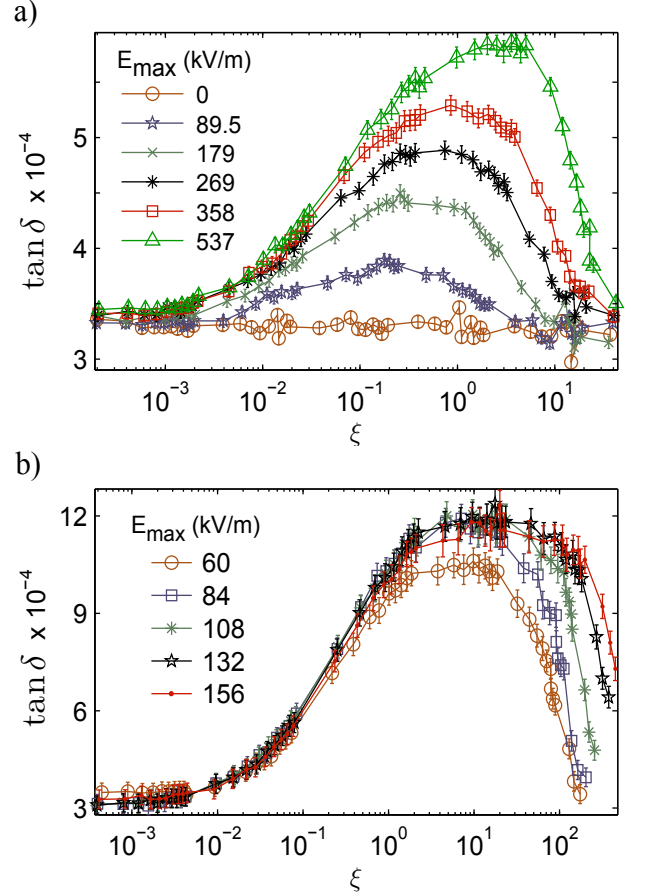


FIG. 3. Dielectric loss tangent as a function of the dimensionless sweep rate ξ , for various maximum values E_{max} of the bias field a) for resonator 1 at $\Omega_{\text{R0}} = 325 \text{ MHz}$ and b) resonator 2 at $\Omega_{\text{R0}} = 50 \text{ MHz}$.

feels the same classical field in every transition, but for $\langle n_{\text{ph}} \rangle \sim 1$ the dynamics of each transition depends on previous transitions of other TLSs. In this regime, calculation of the probability for an absorption of a single photon involves a consideration of multiple emissions and absorptions by an ensemble of TLSs, and thus the interference between many more paths than in the above analysis, where the coherent evolution of a single TLS was considered. It is plausible, however, that most of these paths interfere destructively, justifying an independent treatment of each TLS. In this case, each TLS is described by a Jaynes-Cummings Hamiltonian,

$$\mathcal{H} = \frac{1}{2} \mathcal{E} \sigma_z + \hbar \omega a^\dagger a + g (\sigma_+ a + \sigma_- a^\dagger), \quad (14)$$

which reduces to the LZ Hamiltonian in the vicinity of each resonance. Provided this approximation is justified, the physics discussed above is also applicable in the single-photon regime. This can be verified in Figs. 4, where the data for small photon numbers $\langle n_{\text{ph}} \rangle < 1$ clearly display reduced loss at high sweep rates, suggest-

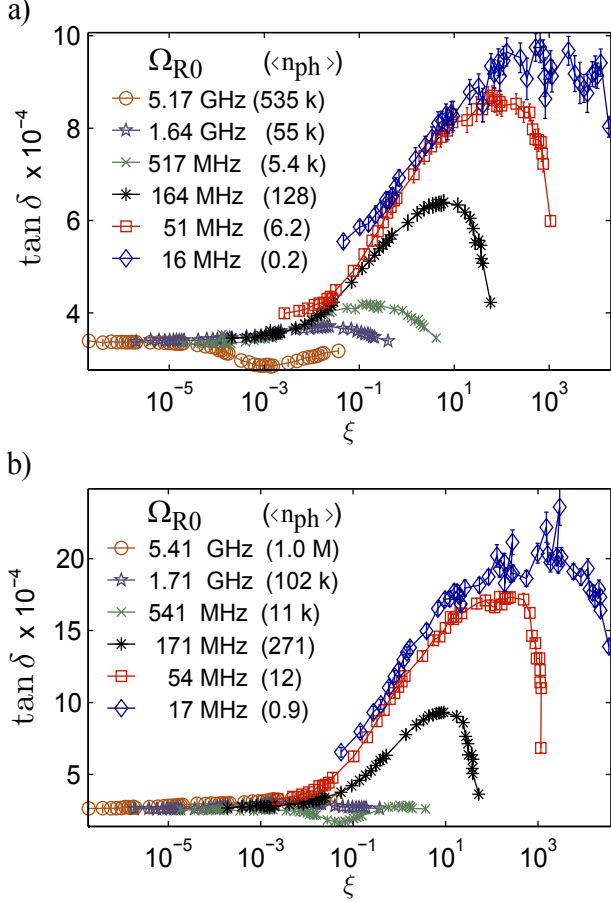


FIG. 4. Dielectric loss tangent as a function of the dimensionless sweep rate ξ for several input powers, corresponding to different field amplitudes E_{ac} . a) for resonator 1 and b) resonator 2, both taken at $E_{max} = 0.9$ MV/m. The legend states the calculated values of Ω_{R0} at $\xi = 0$ and the corresponding mean number of photons in the resonator $\langle n_{ph} \rangle$.

ing that a treatment of independent TLSs is indeed relevant. A more thorough investigation of the single-photon regime will be performed elsewhere.

We note that the single-photon regime is equivalent to the problem of a qubit with energy splitting \mathcal{E}_q coupled to a near-resonant TLS with energy splitting \mathcal{E}_{TLS} . Near resonance the relevant coupling is the transverse one, $\propto \sigma_x^{(q)} \sigma_x^{(TLS)}$, and within the subspace $\{|0, e\rangle, |1, g\rangle\}$ ($|0\rangle, |1\rangle$ and $|g\rangle, |e\rangle$ being the qubit and the TLS ground and excited states, respectively) each resonance is again governed by the LZ dynamics. The above results thus suggest that by sweeping the bias energy of TLSs at a rate larger than their relaxation rate, but smaller than the qubit frequency $\omega_q = \mathcal{E}_q/\hbar$, one may dynamically decouple the qubit from sparse TLSs. Since this sweeping is slow compared to the time scale of the qubit dynamics, the qubit state remains unperturbed. This is in contrast to the saturation regime at strong resonant driving fields, where undesired qubit excitations are inevitable.

ACKNOWLEDGEMENTS

This work was funded by the Deutsche Forschungsgesellschaft (DFG), grant LI2446/1-2. SM acknowledges support from the Minerva foundation. AB acknowledges support from the Helmholtz International Research School for Teratronics (HIRST) and the Landesgraduiertenförderung-Karlsruhe (LGF).

* matityas@post.bgu.ac.il

- [1] G. Wendin, Rep. Prog. Phys. **80**, 106001 (2017).
- [2] C. Neill, P. Roushan, K. Kechedzhi, S. Boixo, S. V. Isakov, V. Smelyanskiy, R. Barends, B. Burkett, Y. Chen, Z. Chen, B. Chiaro, A. Dunsworth, A. Fowler, B. Foxen, R. Graff, E. Jeffrey, J. Kelly, E. Lucero, A. Megrant, J. Mutus, M. Neeley, C. Quintana, D. Sank, A. Vainsencher, J. Wenner, T. C. White, H. Neven, and J. M. Martinis, Science **360**, 195 (2018).
- [3] J. S. Otterbach, R. Manenti, N. Alidoust, A. Bestwick, M. Block, B. Bloom, S. Caldwell, N. Didier, E. Schuyler Fried, S. Hong, P. Karalekas, C. B. Osborn, A. Papageorge, E. C. Peterson, G. Prawiroatmodjo, N. Rubin, C. A. Ryan, D. Scarabelli, M. Scheer, E. A. Sete, P. Sivaram, R. S. Smith, A. Staley, N. Tezak, W. J. Zeng, A. Hudson, B. R. Johnson, M. Reagor, M. P. da Silva, and C. Rigetti, arXiv:1712.05771 (2017).
- [4] P. Day, H.G. LeDuc, B. A. Mazin, A. Vayonakis, and J. Zmuidzinas, Nature (London) **425**, 817 (2003).
- [5] J. Zmuidzinas, Annu. Rev. Condens. Matter Phys. **3**, 169 (2012).
- [6] A. Wallraff, D. I. Schuster, A. Blais, L. Frunzio, R.-S. Huang, J. Majer, S. Kumar, S. M. Girvin, and R. J. Schoelkopf, Nature (London) **431**, 162 (2004).
- [7] J. Q. You and F. Nori, Nature (London) **474**, 589 (2011).
- [8] X. Gu, A. F. Kockum, A. Miranowicz, Y.-X. Liu, and F. Nori, Phys. Rep. **718**, 1 (2017).
- [9] W. A. Phillips, J. Low-Temp. Phys. **7**, 351 (1972).
- [10] P. W. Anderson, B. I. Halperin, and C. M. Varma, Philos. Mag. **25**, 1 (1972).
- [11] C. Müller, J. H. Cole, and J. Lisenfeld, arXiv:1705.01108 (2017).
- [12] J. Lisenfeld, G. J. Grabovskij, C. Müller, J. H. Cole, G. Weiss, and A. V. Ustinov, Nature Comm. **6**, 6182 (2015).
- [13] C. Müller, J. Lisenfeld, A. Shnirman, and S. Poletto, Phys. Rev. B **92**, 035442 (2015).
- [14] S. Meißner, A. Seiler, J. Lisenfeld, A. V. Ustinov, and G. Weiss, Phys. Rev. B **97**, 180505 (2018).
- [15] P. V. Klimov, J. Kelly, Z. Chen, M. Neeley, A. Megrant, B. Burkett, R. Barends, K. Arya, B. Chiaro, Y. Chen, A. Dunsworth, A. Fowler, B. Foxen, C. Gidney, M. Giustina, R. Graff, T. Huang, E. Jeffrey, E. Lucero, J. Y. Mutus, O. Naaman, C. Neill, C. Quintana, P. Roushan, D. Sank, A. Vainsencher, J. Wenner, T. C. White, S. Boixo, R. Babush, V. N. Smelyanskiy, H. Neven, and J. M. Martinis, Phys. Rev. Lett. **121**, 090502 (2018).
- [16] C. Neill, A. Megrant, R. Barends, Y. Chen, B. Chiaro, J. Kelly, J. Y. Mutus, P. J. J. O'Malley, D. Sank, J. Wenner, T. C. White, Y. Yin, A. N. Cleland, and J. M. Martinis, Appl. Phys. Lett. **103**, 072601 (2013).

- [17] J. Burnett, L. Faoro, I. Wisby, V. L. Gurtovoi, A. V. Chernykh, G. M. Mikhailov, V. A. Tulin, R. Shaikhaidarov, V. Antonov, P. J. Meeson, A. Y. Tzalenchuk, and T. Lindström, *Nat. Commun.* **5**, 4119 (2014).
- [18] L. Faoro, and L. B. Ioffe, *Phys. Rev. B* **91**, 014201 (2015).
- [19] A. L. Burin, S. Matityahu, and M. Schechter, *Phys. Rev. B* **92**, 174201 (2015).
- [20] M. Von Schickfus and S. Hunklinger, *Phys. Lett. A* **64**, 144 (1977).
- [21] At the regime of low temperatures $k_B T \ll \hbar\omega$ considered here, the hyperbolic tangent factor is approximately unity, meaning that the thermal excitation of resonant TLSs is negligible.
- [22] A. L. Burin, M. S. Khalil, and K. D. Osborn, *Phys. Rev. Lett.* **110**, 157002 (2013).
- [23] M. S. Khalil, S. Gladchenko, M. J. A. Stoutimore, F. C. Wellstood, A. L. Burin, and K. D. Osborn, *Phys. Rev. B* **90**, 100201(R) (2014).
- [24] L. D. Landau, *Phys. Z. Sov.* **2**, 46 (1932).
- [25] C. Zener, *Proc. R. Soc. Ser. A* **137**, 696 (1932).
- [26] E. C. G. Stückelberg, *Helv. Phys. Acta* **5**, 369 (1932).
- [27] See Supplementary Material for further details of the theory and experiments.
- [28] S. N. Shevchenko, S. Ashhab, and F. Nori, *Phys. Rep.* **492**, 1 (2010).
- [29] E. Shimshoni and Y. Gefen, *Ann. Phys. (N.Y.)* **210**, 16 (1991).
- [30] J. D. Brehm, A. Bilmes, G. Weiss, A. V. Ustinov, and J. Lisenfeld, *Appl. Phys. Lett.* **111**, 112601 (2017).
- [31] S. Probst, F. B. Song, P. A. Bushev, A. V. Ustinov, and M. Weides, *Rev. Sci. Instr.* **86**, 024706 (2015).
- [32] Y. Shalibo, Y. Rofer, D. Shwa, F. Zeides, M. Neeley, J. M. Martinis, and N. Katz, *Phys. Rev. Lett.* **105**, 177001 (2010).
- [33] J. Lisenfeld, C. Müller, J. H. Cole, P. Bushev, A. Lukashenko, A. Shnirman, and A.V. Ustinov, *Phys. Rev. Lett.* **105**, 230504 (2010).
- [34] J. Lisenfeld, A. Bilmes, S. Matityahu, S. Zanker, M. Marthaler, M. Schechter, G. Schön, A. Shnirman, G. Weiss, and A. V. Ustinov, *Sci. Rep.* **6**, 23786 (2016).

Supplementary material for
Dynamical Decoupling of Quantum Two-Level Systems by
Coherent Multiple Landau-Zener Transitions

Shlomi Matityahu,^{1,2} Hartmut Schmidt,³ Alexander Bilmes,³ Alexander Shnirman,^{4,5}
Georg Weiss,³ Alexey V. Ustinov,^{3,6} Moshe Schechter,¹ and Jürgen Lisenfeld³

¹*Department of Physics, Ben-Gurion University of the Negev, Beer Sheva 84105, Israel*

²*Department of Physics, Nuclear Research Centre-Negev, Beer-Sheva 84190, Israel*

³*Physikalisches Institut, Karlsruhe Institute of
Technology (KIT), 76131 Karlsruhe, Germany*

⁴*Institut für Theorie der Kondensierten Materie, KIT, 76131 Karlsruhe, Germany*

⁵*Institute of Nanotechnology, Karlsruhe Institute of Technology,
D-76344 Eggenstein-Leopoldshafen, Germany*

⁶*Russian Quantum Center, National University of
Science and Technology MISIS, Moscow 119049, Russia*

(Dated: June 14, 2022)

I. MODEL

We consider a single TLS with bias energy $\Delta(t) = \Delta(0) - 2\mathbf{p} \cdot \mathbf{E}_{\text{bias}}(t)$ and tunneling energy Δ_0 in a classical single-mode resonator field $\mathbf{E}_{\text{res}}(t) = \mathbf{E}_{\text{ac}} \cos(\omega t)$. Here \mathbf{p} is the TLS dipole moment and $\mathbf{E}_{\text{bias}}(t) \parallel \mathbf{E}_{\text{ac}}$ is a periodic field with period $T_{\text{sw}} \gg \omega^{-1}$. The shortest periods in our experiment are 200 ns, which satisfy the latter condition for microwave resonators with resonance frequency $\omega \approx 2\pi \times 7$ GHz. The Hamiltonian of the isolated TLS (without coupling to a dissipative bath) is

$$\begin{aligned} \mathcal{H} &= \frac{1}{2} (\Delta(t)\sigma_z + \Delta_0\sigma_x) - \mathbf{p} \cdot \mathbf{E}_{\text{ac}} \cos(\omega t)\sigma_z \\ &= \frac{1}{2} \mathcal{E}(t) (\cos \theta(t)\sigma_z + \sin \theta(t)\sigma_x) - \mathbf{p} \cdot \mathbf{E}_{\text{ac}} \cos(\omega t)\sigma_z, \end{aligned} \quad (1)$$

where $\mathcal{E}(t) = \sqrt{\Delta^2(t) + \Delta_0^2}$ is the TLS energy splitting, $\cos \theta(t) = \Delta(t)/\mathcal{E}(t)$ and $\sin \theta(t) = \Delta_0/\mathcal{E}(t)$. We diagonalize the first part of the Hamiltonian by applying the transformation $u(t) = e^{-i\theta(t)\sigma_y/2}$,

$$\mathcal{H}' = u\mathcal{H}u^\dagger + i\hbar\dot{u}u^\dagger = \frac{1}{2}\mathcal{E}(t)\sigma_z - \mathbf{p} \cdot \mathbf{E}_{\text{ac}} \cos(\omega t) (\cos \theta\sigma_z - \sin \theta\sigma_x) - \frac{\hbar\dot{\theta}}{2}\sigma_y. \quad (2)$$

Consider one period of the bias field $t \in [0, T_{\text{sw}}]$. A TLS with $\Delta_0 < \hbar\omega$ is swept through resonance at time t_0 for which $\mathcal{E}(t_0) = \hbar\omega$ (Fig. 1). Near this resonance the energy splitting can be expanded as [1, 2]

$$\mathcal{E}(t) = \sqrt{\Delta^2(t) + \Delta_0^2} \approx \hbar\omega + v(t - t_0), \quad (3)$$

where

$$v = \dot{\mathcal{E}}(t_0) = v_0 \cos \eta \sqrt{1 - \left(\frac{\Delta_0}{\hbar\omega}\right)^2}, \quad (4)$$

with η the angle between the TLS dipole moment and the electric fields and

$$v_0 = 2p\dot{E}_{\text{bias}}(t_0). \quad (5)$$

For the triangular bias field applied in our experiment (see Fig. 1), the sweep velocity is $|v_0| = 4pE_{\text{max}}/T_{\text{sw}}$. From the above definitions one has $\hbar|\dot{\theta}(t_0)| = |\Delta_0 v / (\Delta(t_0)\omega)| = (\Delta_0/\hbar\omega)(v_0/\omega) \cos \eta$. The maximum bias field rate in our experiment is $\dot{E}_{\text{bias}} = 10^{12} \text{ V}/(\text{m}\cdot\text{s})$, which yields $|\dot{\theta}(t_0)|/\omega < 10^{-4}$ (assuming a typical value of $p = 0.5 \text{ e}\text{\AA}$ for the TLS dipole

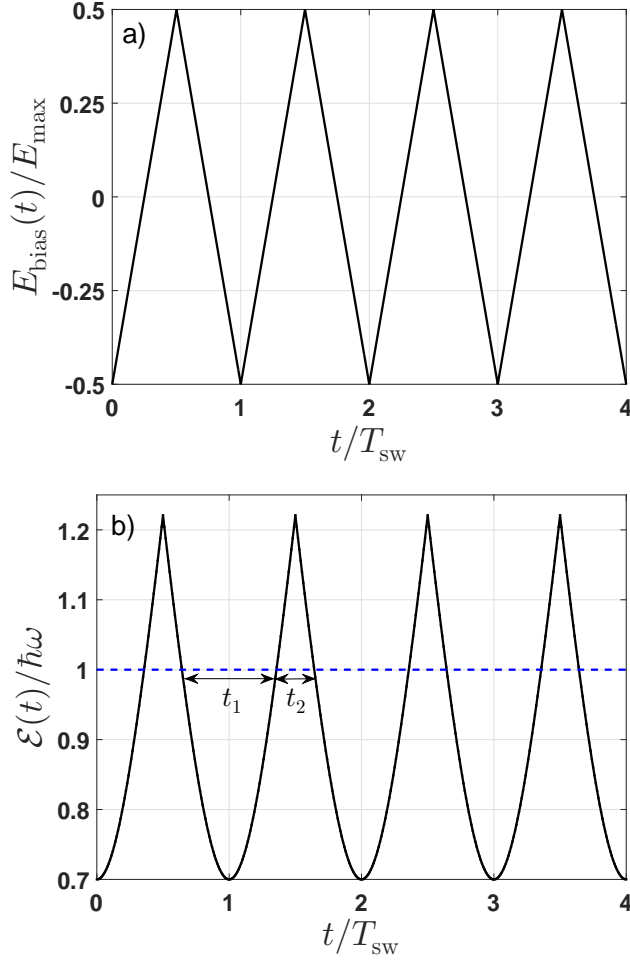


FIG. 1. a) A triangular wave bias field $E_{\text{bias}}(t)$ and b) the corresponding energy splitting $\mathcal{E}(t) = \sqrt{\Delta^2(t) + \Delta_0^2}$ of a TLS with bias energy $\Delta(t) = 0.5 + E_{\text{bias}}(t)$ and tunneling energy $\Delta_0 = 0.7$ (in units of $\hbar\omega$). The intersections of $\mathcal{E}(t)$ with the dashed line correspond to times where the TLS is swept through resonance with the resonator, the dynamics of each resonance is of the LZ type, with the Hamiltonian (9). In each period of the bias field, the time intervals t_1 and t_2 correspond to free propagation between subsequent LZ transitions, with $t_1 + t_2 = T_{\text{sw}}$.

moment). We can therefore safely neglect the last term in Eq. (2). Moreover, near resonance ($\mathcal{E} \approx \hbar\omega$) and for $\Omega_{\text{R}0} \equiv pE_{\text{ac}}/\hbar \ll \omega$, the longitudinal coupling $\propto \sigma_z$ is irrelevant compared to the transverse one $\propto \sigma_x$. As a result, near each resonance the Hamiltonian (2) can be reduced to

$$\mathcal{H}' \approx \frac{1}{2}\mathcal{E}(t)\sigma_z + \hbar\Omega_{\text{R}}\cos(\omega t)\sigma_x, \quad (6)$$

where

$$\Omega_R = \Omega_{R0} \cos \eta \sin \theta \approx \Omega_{R0} \frac{\Delta_0}{\hbar \omega} \cos \eta \quad (7)$$

is the TLS Rabi frequency. Finally, we transform to the rotating frame of reference by applying the transformation $u_R = e^{i\omega t \sigma_z/2}$,

$$\mathcal{H}'_R = u_R \mathcal{H} u_R^\dagger + i\hbar \dot{u}_R u_R^\dagger = \frac{1}{2} (\mathcal{E}(t) - \hbar \omega) \sigma_z + \hbar \Omega_R \cos(\omega t) (\sigma_+ e^{i\omega t} + \sigma_- e^{-i\omega t}), \quad (8)$$

where $\sigma_\pm = (\sigma_x \pm i\sigma_y)/2$. Under the conditions above, the rotating wave approximation can be invoked and the dynamics in the vicinity of each resonance is governed by the Landau-Zener (LZ) Hamiltonian

$$\mathcal{H}'_R \approx \mathcal{H}_{LZ} = \frac{1}{2} v(t - t_0) \sigma_z + \frac{1}{2} \hbar \Omega_R \sigma_x. \quad (9)$$

II. LIOUVILLE SPACE

We work in Liouville space, i.e. the linear space spanned by all linear operators acting on the Hilbert space. In a Hilbert space \mathcal{H}_n of dimension n , the elements are state vectors $|\psi\rangle$ spanned by a set of orthonormal basis states $\{|i\rangle\}_{i=1}^n$, namely $|\psi\rangle = \sum_{i=1}^n c_i |i\rangle$ with $c_i = \langle i|\psi\rangle$. An operator \hat{O} acting on the state vectors can be represented as $\hat{O} = \sum_{i,j=1}^n O_{ij} |i\rangle \langle j|$ with $O_{ij} = \langle i|\hat{O}|j\rangle$. Since any linear combination of these operators is also a linear operator, the set of linear operators $|\hat{O}\rangle$ acting over the Hilbert space with an inner product $\langle \hat{O}_1|\hat{O}_2\rangle = \text{Tr}(\hat{O}_1^\dagger \hat{O}_2)$ forms a linear space known as the Liouville space. This space is spanned by the basis $\{|i\rangle \otimes |j\rangle\}_{i,j=1}^n$ and its dimension is n^2 . Here the basis vector $|i\rangle \otimes |j\rangle$ corresponds to the Hilbert space operator $|i\rangle \langle j|$. Linear operators in Liouville space acting on the elements $|\hat{O}\rangle$ are called superoperators and will be denoted as $\hat{\hat{L}}$.

Let us find the superoperator $\hat{\hat{L}}$ corresponding to the operator $\hat{A}\hat{O}\hat{B}$, i.e. the superoperator $\hat{\hat{L}}$ for which $\hat{\hat{L}}|\hat{O}\rangle = |\hat{A}\hat{O}\hat{B}\rangle$. This is obtained by transforming $\hat{A}\hat{O}\hat{B} = \sum_{i,j,k,l=1}^n A_{ij} O_{jk} B_{kl} |i\rangle \langle l|$ into

$$\begin{aligned} |\hat{A}\hat{O}\hat{B}\rangle &= \sum_{i,j,k,l=1}^n A_{ij} O_{jk} B_{kl} |i\rangle \otimes |l\rangle = \sum_{j,k=1}^n O_{jk} \left(\hat{A} |j\rangle \otimes \hat{B}^T |k\rangle \right) \\ &= \hat{A} \otimes \hat{B}^T \sum_{j,k=1}^n O_{jk} |j\rangle \otimes |k\rangle = \hat{A} \otimes \hat{B}^T |\hat{O}\rangle, \end{aligned} \quad (10)$$

which shows that $\hat{L} = \hat{A} \otimes \hat{B}^T$. For example, a unitary evolution of the density matrix, $\hat{\rho} \rightarrow \hat{\mathcal{U}}\hat{\rho}\hat{\mathcal{U}}^\dagger$, is described in Liouville space as $|\hat{\rho}\rangle \rightarrow \hat{\mathcal{U}} \otimes \hat{\mathcal{U}}^* |\hat{\rho}\rangle$.

Below and in the main text we omit the caret symbol from Hilbert space operators and Liouville space vectors and superoperators. Accordingly, the 2×2 density matrix operator in Hilbert space will be denoted as ρ , and its representation as a 4-vector in Liouville space will be denoted as $|\rho\rangle = (\rho_{00}, \rho_{01}, \rho_{10}, \rho_{11})^T$. The distinction between Hilbert space operators and Liouville space superoperators should be clear by the context.

III. FULL-COUNTING STATISTICS FOR PHOTON ABSORPTION BY A TLS

To calculate the full counting statistics of the photon number absorbed by a TLS after time $t = NT_{\text{sw}}$, we notice that in a fully quantized description of matter and light, the LZ transitions described above are transitions between the diabatic states $|g, n\rangle$ and $|e, n-1\rangle$ of the combined TLS-field system ($|g\rangle$ and $|e\rangle$ being the ground and excited states of the TLS, and $|n\rangle$ being a photon number state). The resonance in this fully quantized picture is shown in Fig. 2, which plots the energy levels of the non-interacting TLS-field Hamiltonian $\mathcal{H}_0 = (\mathcal{E}/2)\sigma_z + \hbar\omega a^\dagger a$ (a^\dagger and a are the photon creation and annihilation operators) as a function of the bias energy Δ . Below we consider the periodic back and forth crossings of one of these resonances.

We insert a counting field k into the evolution operator describing a single LZ transition [3] governed by the Hamiltonian (9),

$$\mathcal{U}_{\text{LZ}}(k) = \begin{pmatrix} \sqrt{P} & e^{i\frac{k}{2}} e^{-i\psi} \sqrt{1-P} \\ -e^{-i\frac{k}{2}} e^{i\psi} \sqrt{1-P} & \sqrt{P} \end{pmatrix}, \quad (11)$$

where $P = e^{-1/\xi}$ is the non-adiabatic transition probability with $\xi = 2|v|/(\pi\hbar\Omega_{\text{R}}^2)$, and $\psi = \pi/4 + \arg \Gamma(1-i/(2\pi\xi)) - [\ln(2\pi\xi) + 1]/(2\pi\xi)$ is the so-called Stokes phase (here Γ is the gamma function) [3]. In the presence of the counting field k , the appropriate superoperator corresponding to the evolution of the density matrix $|\rho\rangle$ is

$$U_{\text{LZ}} = \mathcal{U}_{\text{LZ}}(k) \otimes [\mathcal{U}_{\text{LZ}}(-k)]^*, \quad (12)$$

since the counting field changes sign on the two Keldysh contours. It should be noted that the evolution operator (11) corresponds to the Hamiltonian (9) with positive sign of

the sweep velocity v [3]. Without a counting field, the evolution operator corresponding to the Hamiltonian (9) with negative sign of v is obtained by swapping the off-diagonal elements [3, 5]. Since the exponential terms corresponding to the counting field are not affected by the sign of v , the appropriate transformation for the evolution operator (11) is $\psi \rightarrow \pi - \psi$.

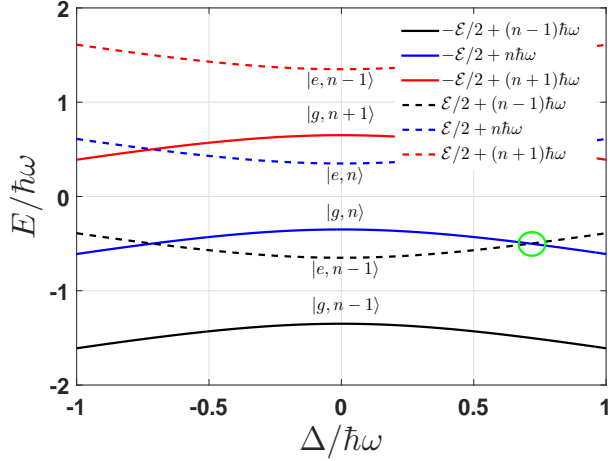


FIG. 2. Energy levels of the non-interacting TLS-field Hamiltonian $\mathcal{H}_0 = (\mathcal{E}/2)\sigma_z + \hbar\omega a^\dagger a$ as a function of the bias energy Δ , for $\Delta_0 = 0.7$ (in units of $\hbar\omega$). The green circle shows the resonance between the states $|g, n\rangle$ and $|e, n-1\rangle$. Subsequent resonances described in Fig. 1 correspond to crossings of this resonance in opposite directions.

In between two successive transitions, the TLS is out of resonance for a time interval t , and its interaction with the resonator ac field is not important. The TLS dynamics within this time interval is described by the Lindblad master equation,

$$\dot{\rho} = -\frac{i}{\hbar} [\mathcal{H}_{\text{TLS}}, \rho] + \sum_{i=\pm} \Gamma_i \left(L_i \rho L_i^\dagger - \frac{1}{2} \{L_i^\dagger L_i, \rho\} \right), \quad (13)$$

where $\mathcal{H}_{\text{TLS}}(t) = (\mathcal{E}(t)/2)\sigma_z$, $L_\pm = \sigma_\pm = (\sigma_x \pm i\sigma_y)/2$ and $\Gamma_+ = \Gamma_\uparrow$, $\Gamma_- = \Gamma_\downarrow$ are the transition rates between the TLS eigenstates. For simplicity, we assume no pure dephasing, such that the decoherence rate is $\Gamma_2 = \Gamma_1/2$, where $\Gamma_1 = \Gamma_\uparrow + \Gamma_\downarrow$ is the relaxation rate. The

components of this master equation read

$$\begin{aligned}
\dot{\rho}_{00} &= -\Gamma_{\downarrow}\rho_{00} + \Gamma_{\uparrow}\rho_{11}, \\
\dot{\rho}_{01} &= -\left(i\frac{\mathcal{E}(t)}{\hbar} - \Gamma_2\right)\rho_{01}, \\
\dot{\rho}_{10} &= \left(i\frac{\mathcal{E}(t)}{\hbar} - \Gamma_2\right)\rho_{10}, \\
\dot{\rho}_{11} &= \Gamma_{\downarrow}\rho_{00} - \Gamma_{\uparrow}\rho_{11}.
\end{aligned} \tag{14}$$

Taking into account that $\text{Tr}[\rho(t)] = \rho_{00}(t) + \rho_{11}(t) = 1$ at any time t , the solution of these equations is $|\rho(t)\rangle = U(t)|\rho(0)\rangle$, with the superoperator

$$U(t) = \begin{pmatrix} \frac{\Gamma_{\uparrow}}{\Gamma_1} + \frac{\Gamma_{\downarrow}}{\Gamma_1}e^{-\Gamma_1 t} & 0 & 0 & \frac{\Gamma_{\uparrow}}{\Gamma_1}(1 - e^{-\Gamma_1 t}) \\ 0 & e^{i\phi(t) - \Gamma_2 t} & 0 & 0 \\ 0 & 0 & e^{-i\phi(t) - \Gamma_2 t} & 0 \\ \frac{\Gamma_{\downarrow}}{\Gamma_1}(1 - e^{-\Gamma_1 t}) & 0 & 0 & \frac{\Gamma_{\downarrow}}{\Gamma_1} + \frac{\Gamma_{\uparrow}}{\Gamma_1}e^{-\Gamma_1 t} \end{pmatrix}, \tag{15}$$

where $\phi(t) = \frac{1}{\hbar} \int_0^t \mathcal{E}(t') dt'$. The evolution of the density matrix after one period of the bias field is given by $|\rho(T_{\text{sw}}, k)\rangle = U_{\text{sw}}(k)|\rho(0)\rangle$, where $U_{\text{sw}}(k) = U_{\text{LZ}}(\pi - \psi, k)U(t_2)U_{\text{LZ}}(\psi, k)U(t_1)$ with $T_{\text{sw}} = t_1 + t_2$. Note that the matrices describing the LZ transitions differ by the Stokes phase, as discussed above, since two subsequent transitions have different sign of velocity [see Fig. 1b)]. Therefore, if the Hamiltonian (9) describes one of the transitions in a period, the second transition will be given by the same Hamiltonian, since both v and σ_z switch signs. The evolution after time $t = NT_{\text{sw}}$ is then

$$|\rho(t, k)\rangle = U_{\text{sw}}^N(k)|\rho(0)\rangle. \tag{16}$$

Letting $p(t, n)$ be the probability of dissipating n photons at time t , we define the generating function

$$\chi(t, k) = \sum_{n=0}^{\infty} e^{ikn} p(t, n), \tag{17}$$

such that the moments of $p(t, n)$ are given by

$$\langle N_{\text{ph}}^m(t) \rangle = \sum_{n=0}^{\infty} n^m p(t, n) = (-i)^m \left. \frac{\partial^m \chi(t, k)}{\partial k^m} \right|_{k=0}. \tag{18}$$

Within the full counting statistics formalism, the generating function is obtained by taking the partial trace over the TLS state,

$$\chi(t, k) = \text{Tr} [|\rho(t, k)\rangle] = \text{Tr} [U_{\text{sw}}^N(k) |\rho(0)\rangle], \quad (19)$$

where the trace operation is defined as $\text{Tr} [|\rho\rangle] \equiv \rho_{00} + \rho_{11}$. The quantity we are interested in is the average number of photons absorbed by the TLS during time $t = NT_{\text{sw}}$,

$$\begin{aligned} \langle N_{\text{ph}}(t) \rangle &= -i \frac{\partial \chi(t, k)}{\partial k} \Big|_{k=0} = -i \frac{d}{dk} \text{Tr} [U_{\text{sw}}^N(k) |\rho(0)\rangle] \Big|_{k=0} \\ &= -i \text{Tr} \left[\frac{d}{dk} U_{\text{sw}}^N(k) \Big|_{k=0} |\rho(0)\rangle \right]. \end{aligned} \quad (20)$$

To calculate this quantity, we write the superoperator $U_{\text{sw}}(k)$ in terms of its eigendecomposition, $U_{\text{sw}}(k) = V_k \Lambda_k G_k$, where $\Lambda(k) = \text{diag}\{\lambda_1(k), \lambda_2(k), \lambda_3(k), \lambda_4(k)\}$ is the diagonal matrix of eigenvalues $\{\lambda_i(k)\}_{i=1}^4$, and $V_k, G_k = V_k^{-1}$ are the matrices whose columns and rows are the corresponding right and left eigenvectors, respectively. We obtain,

$$\begin{aligned} \langle N_{\text{ph}}(t) \rangle &= -i \text{Tr} \left[\frac{d}{dk} (V_k \Lambda_k^N G_k) \Big|_{k=0} |\rho(0)\rangle \right] \\ &= -i \text{Tr} \left[(V'_0 \Lambda_0^N G_0 + N V_0 \Lambda'_0 \Lambda_0^{N-1} G_0 + V_0 \Lambda_0^N G'_0) |\rho(0)\rangle \right]. \end{aligned} \quad (21)$$

In the limit $N \rightarrow \infty$ only the middle term of Eq. (21) will contribute to the photon absorption rate per TLS, $\gamma_{\text{abs}} = \lim_{t \rightarrow \infty} \langle N_{\text{ph}}(t) \rangle / t$, and therefore

$$\gamma_{\text{abs}} = \lim_{t \rightarrow \infty} \frac{\langle N_{\text{ph}}(t) \rangle}{t} = \lim_{N \rightarrow \infty} \frac{\langle N_{\text{ph}}(t = NT_{\text{sw}}) \rangle}{NT_{\text{sw}}} = -\frac{i}{T_{\text{sw}}} \lim_{N \rightarrow \infty} \text{Tr} [V_0 \Lambda'_0 \Lambda_0^{N-1} G_0 |\rho(0)\rangle]. \quad (22)$$

To calculate Eq. (22), one needs to diagonalize a 4×4 matrix. Further analytical progress can be achieved by inserting the identity matrix $G_0 V_0$ into Eq. (20),

$$\gamma_{\text{abs}} = -\frac{i}{T_{\text{sw}}} \lim_{N \rightarrow \infty} \text{Tr} [V_0 \Lambda'_0 G_0 V_0 \Lambda_0^{N-1} G_0 |\rho(0)\rangle]. \quad (23)$$

Since for $k = 0$ we have $\text{Tr} [|\rho(t, k=0)\rangle] = 1$ for any time t , Eq. (16) implies that $\langle g_1| = (1, 0, 0, 1)$ is a left eigenvector of $U_{\text{sw}}(0)$ with eigenvalue $\lambda_1(0) = 1$. For a stationary solution, the other eigenvalues satisfy $|\lambda_i(0)| < 1$ for $i = 2, 3, 4$. Thus, in the limit $N \rightarrow \infty$, $V_0 \Lambda_0^{N-1} G_0$ reduces to $|v_1\rangle \langle g_1|$, where $|v_1\rangle$ is the right eigenvector of $U_{\text{sw}}(k=0)$ corresponding to the eigenvalue $\lambda_1(k=0) = 1$. Hence,

$$\begin{aligned} \gamma_{\text{abs}} &= -\frac{i}{T_{\text{sw}}} \text{Tr} [V_0 \Lambda'_0 G_0 |v_1\rangle \langle g_1| \rho(0)] = -\frac{i}{T_{\text{sw}}} \text{Tr} [V_0 \Lambda'_0 G_0 |v_1\rangle] \\ &= -\frac{i}{T_{\text{sw}}} \langle g_1 | V_0 \Lambda'_0 G_0 | v_1 \rangle. \end{aligned} \quad (24)$$

Finally, we substitute $\Lambda_0 = G_0 U_{\text{sw}}(0) V_0$ to obtain

$$\begin{aligned}\gamma_{\text{abs}} &= -\frac{i}{T_{\text{sw}}} \langle g_1 | V_0 \Lambda'_0 G_0 | v_1 \rangle = -\frac{i}{T_{\text{sw}}} \langle g_1 | V_0 G'_0 U_{\text{sw}}(0) + U'_{\text{sw}}(0) + U_{\text{sw}}(0) V'_0 G_0 | v_1 \rangle \\ &= -\frac{i}{T_{\text{sw}}} \langle g_1 | \frac{dU_{\text{sw}}}{dk} \Big|_{k=0} | v_1 \rangle ,\end{aligned}\quad (25)$$

where in the last step we have used the fact that $|v_1\rangle$ and $\langle g_1|$ are right and left eigenvectors of $U_{\text{sw}}(0)$ corresponding to an eigenvalue $\lambda_1(0) = 1$, and $V_0 G'_0 + V'_0 G_0 = \frac{d}{dk} (V_k G_k) \Big|_{k=0} = 0$.

IV. TLS PHOTON ABSORPTION RATE AND DIELECTRIC LOSS TANGENT

The evaluation of Eq. (25) involves a calculation of the derivative $dU_{\text{sw}}/dk|_{k=0}$ and the right eigenvector $|v_1\rangle$ of $U_{\text{sw}}(0)$ corresponding to an eigenvalue $\lambda_1(0) = 1$, and can therefore be done analytically. At low temperatures $k_B T \ll \hbar\omega$ one has $\Gamma_\uparrow \ll \Gamma_\downarrow$ (and thus $\Gamma_1 \approx \Gamma_\downarrow$), and we end up with $\gamma_{\text{abs}} = a/b$, where

$$\begin{aligned}a &= (P-1) \left\{ 4(1-P) \sinh\left(\frac{\Gamma_1 t_2}{1}\right) \sinh\left(\frac{\Gamma_1 t_2}{2}\right) \cos(\tilde{\phi}_1 - \tilde{\phi}_2) + \right. \\ &2P \sinh\left(\frac{\Gamma_1 T_{\text{sw}}}{2}\right) \left[\sinh\left(\frac{\Gamma_1 t_2}{2}\right) \cos \tilde{\phi}_1 + \sinh\left(\frac{\Gamma_1 t_1}{2}\right) \cos \tilde{\phi}_2 \right] + 2P - 1 - \cosh(\Gamma_1 T_{\text{sw}}) + \\ &\left. [\cosh(\Gamma_1 t_1) + \cosh(\Gamma_1 t_2)] (1-P) \right\}, \\ b &= 2T_{\text{sw}} \left\{ \frac{1}{4} \sinh(\Gamma_1 T_{\text{sw}}) + \frac{1}{2} \sinh\left(\frac{\Gamma_1 T_{\text{sw}}}{2}\right) \cos(\tilde{\phi}_1 - \tilde{\phi}_2) (2P-1) + \right. \\ &P(P-1) \left[\sinh\left(\frac{\Gamma_1 t_1}{2}\right) \cos \tilde{\phi}_1 + \sinh\left(\frac{\Gamma_1 t_2}{2}\right) \cos \tilde{\phi}_2 \right] - \\ &\left. \sinh\left(\frac{\Gamma_1 T_{\text{sw}}}{2}\right) P^2 (\cos \tilde{\phi}_1 + \cos \tilde{\phi}_1) \right\},\end{aligned}\quad (26)$$

with $\tilde{\phi}_1 = \phi_1 - 2\psi$ and $\tilde{\phi}_2 = \phi_2 + 2\psi$. Note that the absorption rate γ_{abs} depends on the parameters $\Delta(0)$, Δ_0 and η of each TLS, via its dependence on P , Γ_1 , t_1 , ϕ_1 , ϕ_2 and ψ .

The expression relating the dielectric loss tangent to the total photon absorption rate per unit volume, Γ_{abs} , is obtained by comparing the equivalent expressions for the power dissipation energy, $P_{\text{dis}} = -\hbar\omega\Gamma_{\text{abs}} = -\frac{1}{2}\omega\epsilon''E_{\text{ac}}^2$. This gives

$$\tan \delta = \frac{\epsilon''}{\epsilon'} = \frac{2\hbar\Gamma_{\text{abs}}}{\epsilon E_{\text{ac}}^2} = \frac{2p^2\Gamma_{\text{abs}}}{\epsilon\hbar\Omega_{\text{R0}}^2}.\quad (27)$$

The total absorption rate per unit volume is obtained by averaging over the distribution of TLSs and the orientation of their dipole moments, as follow. For a given value of $\Delta_0 < \hbar\omega$

and η , the TLSs that are swept into resonance are those with bias energy $\Delta(0)$ in the window $2pE_{\max}|\cos\eta|$ around $\sqrt{(\hbar\omega)^2 - \Delta_0^2}$. The total photon absorption rate per unit volume is thus

$$\Gamma_{\text{abs}} = \int d^2n_{\text{TLS}} \gamma_{\text{abs}}(\Delta(0), \Delta_0, \eta) = 2pE_{\max} \int_0^{\hbar\omega} d\Delta_0 \frac{P_0}{\Delta_0} \int_0^\pi d\eta \frac{\sin\eta}{2} |\cos\eta| \gamma_{\text{abs}}(\Delta_0, \eta), \quad (28)$$

where $d^2n_{\text{TLS}} = (P_0/\Delta_0) d\Delta d\Delta_0$ is the number of TLSs per unit volume with bias and tunneling energies in an element $d\Delta d\Delta_0$ around (Δ, Δ_0) . In the last step of Eq. (28) we assumed that γ_{abs} is independent of $\Delta(0)$ so that the integral over the bias energy becomes trivial.

In the incoherent limit $\Gamma_1 T_{\text{sw}} \gg 1$, or $\xi \ll \xi_2$ with $\xi_2 \equiv 8pE_{\max}\Gamma_1/(\pi\hbar\Omega_{\text{R}0}^2)$, we have $a \approx (1-P) \cosh(\Gamma_1 T_{\text{sw}}) \approx (1-P) e^{\Gamma_1 T_{\text{sw}}/2}$ and $b \approx T_{\text{sw}} \sinh(\Gamma_1 T_{\text{sw}})/2 \approx T_{\text{sw}} e^{\Gamma_1 T_{\text{sw}}/4}$ in the leading order. Thus,

$$\gamma_{\text{abs}} \approx \frac{2(1-P)}{T_{\text{sw}}}, \quad (29)$$

which is independent of $\Delta(0)$. Using Eq. (28), the loss tangent (27) takes the form

$$\begin{aligned} \tan\delta &\approx \frac{2P_0 p^2 v_0}{\epsilon \hbar \Omega_{\text{R}0}^2} \int_0^{\hbar\omega} \frac{d\Delta_0}{\Delta_0} \int_0^\pi d\eta \frac{\sin\eta}{2} |\cos\eta| \left(1 - e^{-\pi\hbar\Omega_{\text{R}}^2/2|v|}\right) \\ &= \frac{2P_0 p^2}{\epsilon \hbar} \int_0^{\hbar\omega} \frac{d\Delta_0}{\Delta_0} \frac{(\Delta_0/\hbar\omega)^2}{\sqrt{1 - (\Delta_0/\hbar\omega)^2}} \int_0^\pi d\eta \frac{\sin\eta}{2} \cos^2\eta \frac{|v|}{\Omega_{\text{R}}^2} \left(1 - e^{-\pi\hbar\Omega_{\text{R}}^2/2|v|}\right), \end{aligned} \quad (30)$$

where in the last step we have used Eqs. (4) and (7). Equation (30) is analogous to Eq. (6) of Ref. 1, and reduces in the non-adiabatic limit $|v| \gg \hbar\Omega_{\text{R}}^2$ to the intrinsic loss tangent $\tan\delta_0 = \pi P_0 p^2/(3\epsilon)$ obtained at low powers. This is readily observed by expanding the exponent in Eq. (30) to first order,

$$\tan\delta \approx \frac{\pi P_0 p^2}{2\epsilon} \int_0^{\hbar\omega} \frac{d\Delta_0}{\Delta_0} \frac{(\Delta_0/\hbar\omega)^2}{\sqrt{1 - (\Delta_0/\hbar\omega)^2}} \int_0^\pi d\eta \sin\eta \cos^2\eta = \frac{\pi P_0 p^2}{3\epsilon}. \quad (31)$$

An analytical evaluation of the loss tangent in the coherent regime $\Gamma_1 T_{\text{sw}} \ll 1$ using the full dependence of Eq. (26) on the parameters $\Delta(0)$, Δ_0 and η is very complicated. To analyze the absorption rate in this regime, we neglect the distribution of the sweep rate v , the Rabi frequency Ω_{R} , the relaxation rate Γ_1 and the dipole moment p , and assume $t_1 = t_2 = T_{\text{sw}}/2$. In terms of the number of coherent transitions, $M = (\Gamma_1 T_{\text{sw}})^{-1} = \xi/\xi_2$, the

numerator and denominator of the absorption rate $\gamma_{\text{abs}} = a/b$ [Eq. (26)] then become

$$\begin{aligned}
a &= (P-1) \left\{ 4 \sinh^2 \left(\frac{1}{4M} \right) (1-P) \cos(\tilde{\phi}_1 - \tilde{\phi}_2) + 2P - 1 - \cosh \left(\frac{1}{M} \right) \right. \\
&\quad \left. + 2 \sinh \left(\frac{1}{4M} \right) \sinh \left(\frac{1}{2M} \right) P (\cos \tilde{\phi}_1 + \cos \tilde{\phi}_2) + 2 \cosh \left(\frac{1}{2M} \right) (1-P) \right\}, \\
b &= \frac{2}{\Gamma_1 M} \left\{ P \left[\sinh \left(\frac{1}{4M} \right) (P-1) (\cos \tilde{\phi}_1 + \cos \tilde{\phi}_2) - \sinh \left(\frac{1}{2M} \right) P \cos \tilde{\phi}_1 \cos \tilde{\phi}_2 \right] \right. \\
&\quad \left. + \frac{1}{2} \sinh \left(\frac{1}{2M} \right) (2P-1) \cos(\tilde{\phi}_1 - \tilde{\phi}_2) + \frac{1}{4} \sinh \left(\frac{1}{M} \right) \right\}. \tag{32}
\end{aligned}$$

The absorption rate $\gamma_{\text{abs}} = a/b$ is then a function of ξ , ξ_2 , $\tilde{\phi}_1$ and $\tilde{\phi}_2$. Figure 1 in the main text shows the loss tangent obtained by averaging the absorption rate over a homogeneous distribution of the phases ϕ_1 and ϕ_2 (and thus of $\tilde{\phi}_1$ and $\tilde{\phi}_2$),

$$\langle \gamma_{\text{abs}} \rangle (\xi, \xi_2) = \frac{1}{(2\pi)^2} \int_0^{2\pi} \int_0^{2\pi} \gamma_{\text{abs}}(\xi, \xi_2, \tilde{\phi}_1, \tilde{\phi}_2) d\tilde{\phi}_1 d\tilde{\phi}_2. \tag{33}$$

To understand the behavior of this average, we consider the coherent regime $M \gg 1$ ($\xi \gg \xi_2$), distinguishing between the adiabatic ($\xi \ll 1$) and non-adiabatic ($\xi \gg 1$) limits. In the coherent and adiabatic limit $\xi_2 \ll \xi \ll 1$, we expand a and b in $1/M$ and P to obtain

$$\gamma_{\text{abs}} \approx \frac{\Gamma_1}{2} \frac{1 - \cos(\tilde{\phi}_1 - \tilde{\phi}_2) + f_1(\tilde{\phi}_1, \tilde{\phi}_2)P}{1 - \cos(\tilde{\phi}_1 - \tilde{\phi}_2) + f_1(\tilde{\phi}_1, \tilde{\phi}_2)P + f_2(\tilde{\phi}_1, \tilde{\phi}_2)(1/M)^2}, \tag{34}$$

where $f_1(\tilde{\phi}_1, \tilde{\phi}_2) = 2 \cos(\tilde{\phi}_1 - \tilde{\phi}_2) - \cos \tilde{\phi}_1 - \cos \tilde{\phi}_2$ and $f_2(\tilde{\phi}_1, \tilde{\phi}_2) = 1/6 - (1/24) \cos(\tilde{\phi}_1 - \tilde{\phi}_2)$. Hence, $\gamma_{\text{abs}} \approx \Gamma_1/2$ with weak dependence on the phases $\tilde{\phi}_1$ and $\tilde{\phi}_2$. This gives rise to loss tangent $\tan \delta \propto \tan \delta_0 \cdot \xi_2$. Physically, in this regime the probability of photon absorption\emission in each transition is $1 - P \approx 1$, so that photons are absorbed and reemitted by the TLS, thus dissipated at a rate $\propto \Gamma_1$.

In the coherent and non-adiabatic limit $\xi \gg 1, \xi_2$, we expand a and b in $1/M$ and $1 - P$ to obtain

$$\gamma_{\text{abs}} \approx \frac{\Gamma_1}{2} \frac{(1-P) (2 - \cos \tilde{\phi}_1 - \cos \tilde{\phi}_2)}{1 - \cos(\tilde{\phi}_1 + \tilde{\phi}_2) + g_1(\tilde{\phi}_1, \tilde{\phi}_2)(1-P) + g_2(\tilde{\phi}_1, \tilde{\phi}_2)(1/M)^2}, \tag{35}$$

where $g_1(\tilde{\phi}_1, \tilde{\phi}_2) = 2 \cos(\tilde{\phi}_1 + \tilde{\phi}_2) - \cos \tilde{\phi}_1 - \cos \tilde{\phi}_2$ and $g_2(\tilde{\phi}_1, \tilde{\phi}_2) = 2/3 - (13/24) \cos(\tilde{\phi}_1 + \tilde{\phi}_2)$. We observe that a resonance occurs at $\tilde{\phi}_1 + \tilde{\phi}_2 = \phi_1 + \phi_2 = 2\pi n$, where n is an integer. Outside this resonance, Eq. (35) yields $\gamma_{\text{abs}}^{\text{non-res}} \propto \Gamma_1(1-P) \approx \Gamma_1/\xi$, with weak dependence on the phases $\tilde{\phi}_1$ and $\tilde{\phi}_2$. We now evaluate the contribution of the resonance. According to Eq. (35),

the resonance width is $\delta\phi \propto \max\{\sqrt{1-P}, 1/M\}$, i.e. $\delta\phi \propto \sqrt{1-P}$ for $M^2(1-P) > 1$ ($\xi > \xi_2^2$) and $\delta\phi \propto 1/M$ for $M^2(1-P) < 1$ ($\xi < \xi_2^2$). The contribution of this resonance to the averaged absorption rate can therefore be estimated as

$$\gamma_{\text{abs}}^{\text{res}} \approx \gamma_{\text{abs}}(\tilde{\phi}_1 = -\tilde{\phi}_2) \cdot \delta\phi \propto \Gamma_1 \begin{cases} \sqrt{1-P} \approx 1/\sqrt{\xi} & M^2(1-P) > 1 \\ M(1-P) \approx 1/\xi_2 & M^2(1-P) < 1 \end{cases}. \quad (36)$$

Note that in both cases $\gamma_{\text{abs}}^{\text{res}} > \gamma_{\text{abs}}^{\text{non-res}}$, so that the contribution of the resonance is the dominant one.

The above analysis reveals the following qualitative behavior in the coherent regime $\xi \gg \xi_2$. For $\xi_2 \ll 1$ the loss tangent behaves as

$$\frac{\tan \delta}{\tan \delta_0} \propto \begin{cases} \xi & \xi \ll \xi_2 \\ \xi_2 & \xi_2 \ll \xi \ll 1, \\ \xi_2/\sqrt{\xi} & \xi \gg 1 \end{cases}, \quad (37)$$

whereas for $\xi_2 \gg 1$

$$\frac{\tan \delta}{\tan \delta_0} \propto \begin{cases} \xi & \xi \ll 1 \\ 1 & 1 \ll \xi \ll \xi_2 \\ 1 & \xi_2 \ll \xi \ll \xi_2^2 \\ \xi_2/\sqrt{\xi} & \xi \gg \xi_2^2 \end{cases}. \quad (38)$$

Note that for $\xi_2 \gg 1$ the scale that governs the decrease in loss tangent is $\propto \xi_2^2$, in agreement with the numerical calculation shown in Fig. 1 in the main text.

V. EXPERIMENTAL DETAILS

A. Setup

The sample was measured in an Oxford Kelvinox 100 dilution refrigerator at a temperature of 30 mK. The sample chip is installed in a light-tight aluminum housing surrounded by a cryoperm magnetic shield. To enable measurements of the resonator in the single-photon regime, the microwave circuitry is heavily filtered and attenuated as illustrated in Fig. 3.

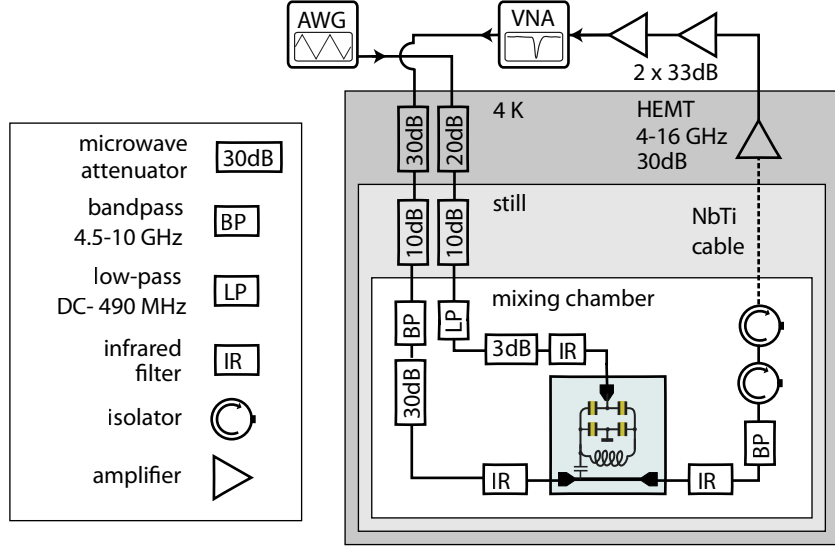


FIG. 3. Setup schematic. Resonator loss is measured by a Vector Network Analyzer (VNA). Thermal isolation of coax cables and noise protection is provided by attenuators thermally anchored to different temperature stages, band-pass (BP) and low-pass filters (LP) (Mini-Circuits), and custom-made infrared filters (IR). After interacting with the sample, the signal passes through two magnetically shielded isolators (QuinStar QCY-060400CM00), a high-mobility electron transistor (HEMT) (Low-Noise Factory LNF-LNC4-16A) and two room-temperature amplifiers (Mini-Circuits VA-183-S). The electric bias to the resonator dielectric is provided by an arbitrary waveform generator (Tektronix AWG 5914B, 1.2 GS/s), generating symmetric triangular waveforms of minimal duration 10ns and 4V amplitude.

B. Sample fabrication

Samples are fabricated in three optical lithography steps. First, a 50 nm thick layer of aluminum is deposited at a rate of 1 nm/s on a cleaned sapphire substrate using an electron beam evaporation system (Plassys MEB 550 S). This layer is patterned into ground plane, transmission line, and resonator inductances using S1805 photoresist, AZ-developer, and reactive-ion etching in a ICP machine (Oxford 100 ICP 180), before stripping the remaining photoresist with NEP. We preferred to etch the first layer over a lift-off process to avoid contamination of the substrate-metal interface by photoresist residuals, while further lithography steps are done by a lift-off process to avoid the first layer to be damaged by

Resonator	f_{res} (GHz)	w_{cap}	Q_c (10^3)	d_{coup}
1	6.892	$5\text{ }\mu\text{m}$	12.8 ± 0.7	$40\text{ }\mu\text{m}$
2	6.952	$7\text{ }\mu\text{m}$	3.4 ± 0.3	$18\text{ }\mu\text{m}$
3	7.71	$5\text{ }\mu\text{m}$	33 ± 9	$100\text{ }\mu\text{m}$

TABLE I. Resonators parameters: measured resonance frequency f_{res} , lateral size of square capacitors w_{cap} , coupling distance to transmission line d_{coup} , and coupling quality factor Q_c .

etching. AZ developer was used because we found that it produces less defects in underlying aluminum films compared to MF319 developer.

In the second lithography step, prior to deposition of the capacitor dielectric, the native aluminum oxide on the bottom capacitor electrodes is removed using an argon ion mill [4]. The aluminum oxide is then deposited at a rate of 0.3 nm/s by aluminum evaporation while the vacuum chamber is exposed to an oxygen flow of 5 sccm , and afterwards covered with a 30 nm thick top layer of aluminum. In a third lithography step, after initial ion-milling removal of the native aluminum oxide, the vias which electrically connect bottom and top metallic layers [see Fig. 2a) in the main text] are formed by placing a 50 nm -thick layer of aluminum as a bandage overlapping both layers.

C. Sample parameters

Table I describes the sample parameters of three different resonators.

VI. ADDITIONAL DATA

Figure 4 shows additional data for resonator 1 [cf. Fig. 3a) in the main text].

-
- [1] A. L. Burin, M. S. Khalil, and K. D. Osborn, Phys. Rev. Lett. **110**, 157002 (2013).
 - [2] M. S. Khalil, S. Gladchenko, M. J. A. Stoutimore, F. C. Wellstood, A. L. Burin, and K. D. Osborn, Phys. Rev. B **90**, 100201(R) (2014).

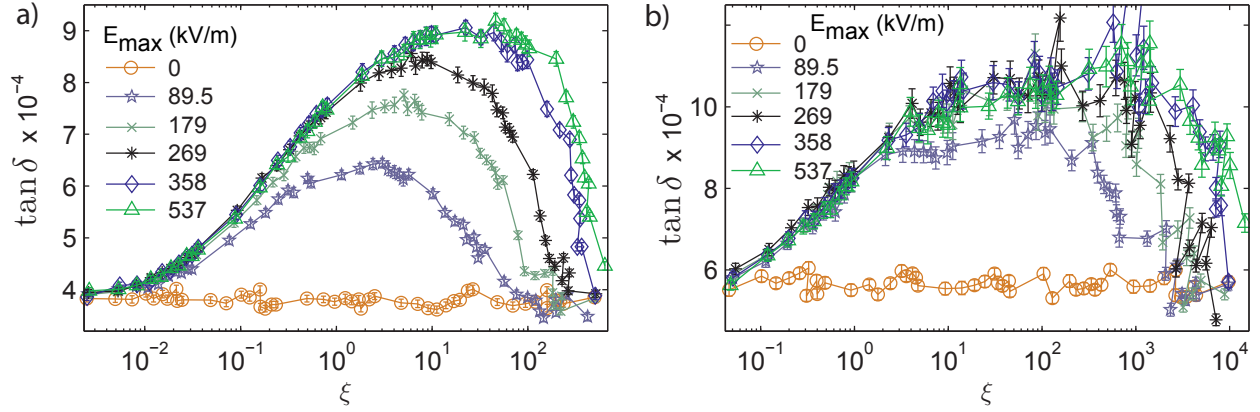


FIG. 4. Dielectric loss tangent of resonator 1 as a function of the dimensionless sweep rate ξ for various maximum values E_{\max} of the bias field. a) applied power -110 dBm, $\Omega_{R0} = 103$ MHz and b) applied power -120 dBm, $\Omega_{R0} = 32.7$ MHz.

- [3] S. N. Shevchenko, S. Ashhab, and F. Nori, Phys. Rep. **492**, 1 (2010).
- [4] L. Grünhaupt, U. von Lüpke, D. Gusenkova, S. T. Skacel, N. Maleeva, S. Schlör, A. Bilmes, H. Rotzinger, A. V. Ustinov, M. Weides and I. M. Pop, Appl. Phys. Lett **111**, 072601 (2017).
- [5] This can be readily shown using the identity $e^{-\alpha\sigma_z+\beta\sigma_x} = e^{\sigma_x(\alpha\sigma_z+\beta\sigma_x)\sigma_x} = \sigma_x e^{\alpha\sigma_z+\beta\sigma_x}\sigma_x$. Since the diagonal elements of the evolution operator (11) are identical, reversing the sign of v in the Hamiltonian (9) amounts to transposing the evolution operator (for $k = 0$, i.e., in the absence of the counting field).